CHAPTER 8

NANO-SIZE PEROVSKITE CATALYST SYNTHESISED BY REACTIVE GRINDING FOR DIESEL SOOT OXIDATION

8.1 Introduction

Several perovskite-type mixed oxides have long been recognized as very active oxidation/reduction catalysts with many potential applications in environmental catalysis [Mishra and Prasad 2014] , generally prepared by citric acid SG method which results a low specific surface area. To increase the surface area, several techniques are developed, mechano-chemical synthesis also known as reactive grinding (RG) has the potential to provide more sustainable solvent-free preparative route to obtain perovskite phase at room temperature, with surface area as high as 100 m^2/g [Uchisavwa et al. 2000]. Following this technique, the double substituted $La_{0.9}Sr_{0.1}Fe_{0.5}Co_{0.5}O_{3-\delta}$ perovskite catalyst was synthesized by reactive grinding using the individual components of simple oxide of each cation as the reactants using ZnO as grinding additive. Thus, the aim of this work was to prepare double substituted $La_{0.9}Sr_{0.1}Fe_{0.5}Co_{0.5}O_{3-\delta}$ via SG and RG methods and compare their textural properties as well as activity for diesel soot oxidation. This chapter also brings in picture the feasibility of RG technique and the effect of operating parameters on diesel soot oxidation.

8.2 Material and Methods

8.2.1 Catalyst Preparation

$La_{0.9}Sr_{0.1}Co_{0.5}Fe_{0.5}O_{3-\delta}$ was prepared by the citric acid sol-gel method, as discussed in section 3.6.1 using nitrate precursors of the constituent elements. $La_{0.9}Sr_{0.1}Co_{0.5}Fe_{0.5}O_{3-\delta}$ was also prepared by reactive grinding using oxide precursors of the constituent elements. The oxide precursors were first calcined at 600 ^{o}C in order to eliminate any possible hydroxides associated with them. 6.16 g of pre-purified La_2O_3, 1.68 g of Co_3O_4, 1.68 g of Fe_2O_3 and 0.44 g of SrO were premixed by hand grinding for 5 min and loaded in a zirconia grinding jar (100 cm^3) with zirconia balls (3 balls of 11 mm size, 4 balls of 9 mm size and 7 balls of 7mm size). The weight ratio of ball to powder was 5:1. The jar was closed with a lid and sealed with O-ring. The revolution per minute (rpm) of jar was kept at 375. The milling was carried out for 4 h under air in planetary ball mill. After this step the perovskite phase was obtained with small impurities of La_2O_3 [Kaliaguine et al. 2001]. Further, the grinding was done for 20 h in two separate jars first without ZnO additive and second with ZnO additive in order to increase the specific surface area [Kaliaguine et al. 2001, Zhou el al. 2010]. The additive was in a weight ratio of perovskite/ZnO = 1. Then the obtained powder was repeatedly washed with diluted NH_4NO_3 in order to leach the additive ZnO from the sample. Finally, the perovskite was calcined in air at 550^{o}C for 4 h. Nomenclature of the prepared catalysts are given in table 8.1.

Table 8.1 Nomenclature of the Catalysts

Catalyst (Preparation method)	**Name**
$La_{0.9}Sr_{0.1}Co_{0.5}Fe_{0.5}O_{3-\delta}$ (SG)	Cat-CC
$La_{0.9}Sr_{0.1}Co_{0.5}Fe_{0.5}O_{3-\delta}$ (RG)	Cat-RG
$La_{0.9}Sr_{0.1}Co_{0.5}Fe_{0.5}O_{3-\delta}$ (RG + ZnO)	Cat-RGA

8.2.2 Catalyst Characterization

The textural characterization of the catalysts was carried out by low temperature N_2-physisorption method using a Micromeritics ASAP 2020 analyser. Phase identification of the catalysts was done by X-ray diffraction (XRD) patterns recorded on a powder X-ray diffractometer (Rigaku Ultima IV) using CuKα1 (λ = 1.5405 Å) radiation with a nickel filter operating at 40mA and 40kV. The XPS measurement was performed on an Amicus spectrometer equipped with Mg Kα X-ray radiation. For typical analysis, the source was operated at a voltage of 15 kV and current of 12 mA. Pressure in the analysis chamber was less than 10^{-5} Pa. The binding energy scale was calibrated by setting the main C 1s line of adventitious impurities at 284.7 eV, giving an uncertainty in peak positions of ±0.2 eV. FTIR spectra of the catalysts were recorded in the range of 400-4000 cm^{-1} on Shimadzu 8400 FTIR spectrometer with KBr pellets at room temperature. Scanning electron micrographs (SEM) and SEM EDX were recorded on Zeiss EVO 18 scanning electron microscope (SEM) instrument. An accelerating voltage of 15kV and magnification of 1000X was applied.

8.2.3 Activity measurement of the Catalysts

The catalytic performances of the prepared catalysts for oxidation of soot were evaluated in a compact fixed bed tubular quartz reactor as shown in figure 3.9 and discussed in the section 3.6.2.

8.3 Results and Discussion

8.3.1 Textural Characterization by N_2-Physisorption

Typical nitrogen physisorption isotherms and pore size distribution curves for the catalysts Cat-CC and Cat-RGA are shown in Figures 7.1 and 7.2 respectively. The nitrogen sorption isotherms exhibit type-IV isotherms with H1 type hysteresis loop.

This type of isotherm occurs on porous adsorbent with pores in the mesoporous range of 2-25 nm. The desorption curves are practically coincide with adsorption branch of the respective sorption isotherms of all the samples irrespective of the composition of the catalysts. This behavior is a representative of open textured pores, which offers practically negligible diffusion resistance during the reaction. The pore size distribution curve for Cat-CC presented in figure 7.1 (b) shows wide distribution having trimodal nature with most probable pores around 40, 140, 220 Å while for Cat-RGA shown in figure 7.2 (b) it is narrowly distributed monomodal with most probable pore around 70 Å.

The textural properties including BET surface area, total pore volume and average pore diameter of the perovskites studied in the present investigation are summarized in Table 8.2. It can be seen from the table that the SG-prepared perovskite catalyst have a low specific surface area (7.29 m^2/g). Cat-RG synthesized without additive possessed higher surface area (32.6 m^2/g) and smaller crystallites than samples prepared by SG method. Cat-RGA prepared with ZnO additive exhibited the highest surface area (92.5 m^2/g), smallest crystallites (10.4 nm).

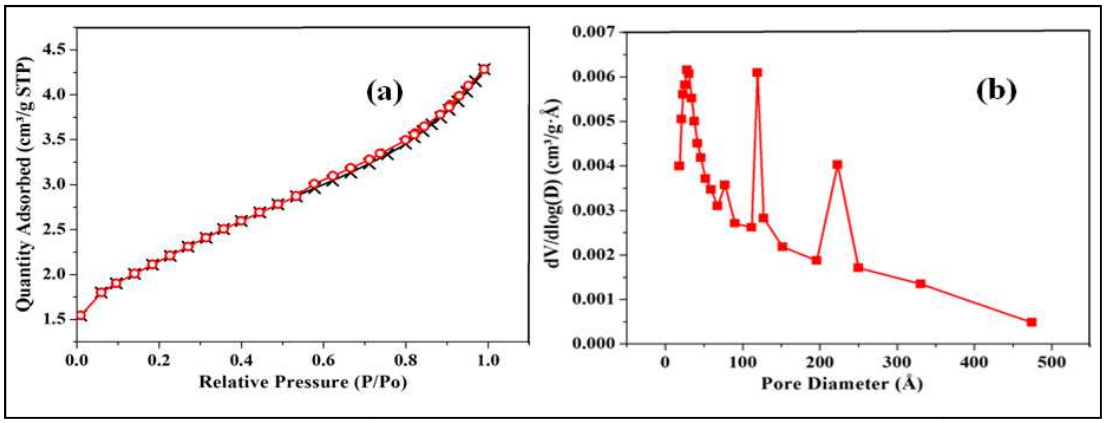

Figure 8.1 Cat-CC (a) N_2 adsorption/desorption isotherms and (b) pore size distribution curves

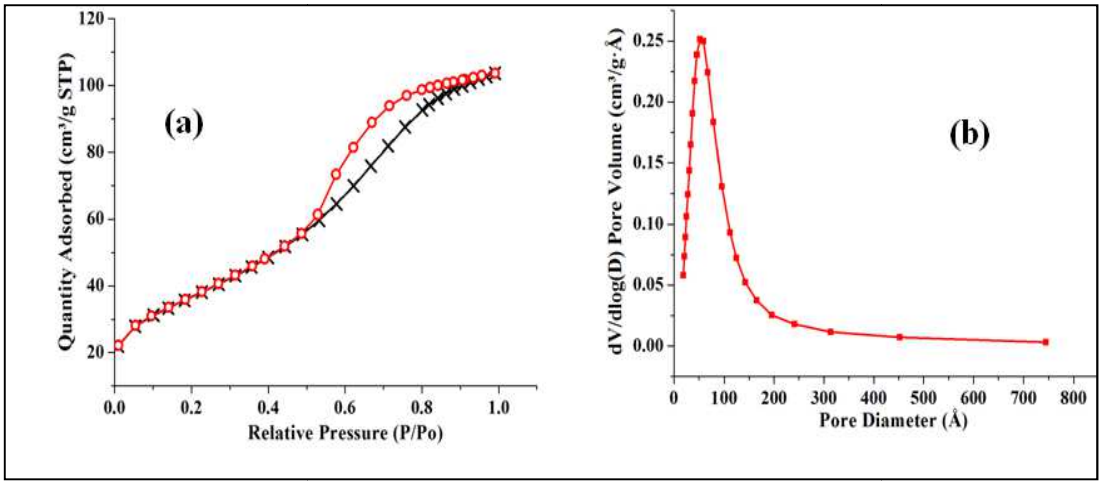

Figure 8.2 Cat-RGA (a) N_2 sorption/desorption isotherms, (b) pore size distribution curves

Table 8.2 Surface area, average pore diameter and crystallite size data

Catalyst	Surface area (m^2/g)	Average pore diameter (Å)	Crystallite size (nm)
Cat-CC	7.29	06.24	14.09
Cat-RG	32.60	7.72	14.80
Cat-RGA	92.50	8.04	10.40

8.3.2 XRD Analysis of the Catalysts

The powder XRD patterns of catalyst samples are shown in Figure 8.3. The XRD peaks were found to be very sharp indicating that the ABO_3 perovskite structure which is well maintained in all the samples. The XRD analysis of SG-prepared Cat-CC showed the formation of cubic $LaFeO_3$ structure (JCPDS card 00-075-0439) and $LaCoO_3$ (JCPDS card No. 25-1060) with no traces of other phase. In the RG- Prepared Cat-RG and Cat-RG-ZnO other phases such as Fe_2O_3 (JCPDS card 00-001-1053) and La_2O_3 (JCPDS card 00-005-0602) were detected in addition to the major ABO_3 perovskite phase. The diffractogram of Cat-RGA was scattered in many directions leading to a large bump distributed in a wide range instead of high intensity narrower peaks present in Cat-CC

and Cat-RG. Peak broadening is normally seen in nano crystallites smaller than 100 nm. The crystallite size was estimated using the Scherrer equation and are reported in Table 8.2. The Cat-RGA shows the smallest crystallite size of 10.4 nm in comparison to other catalysts.

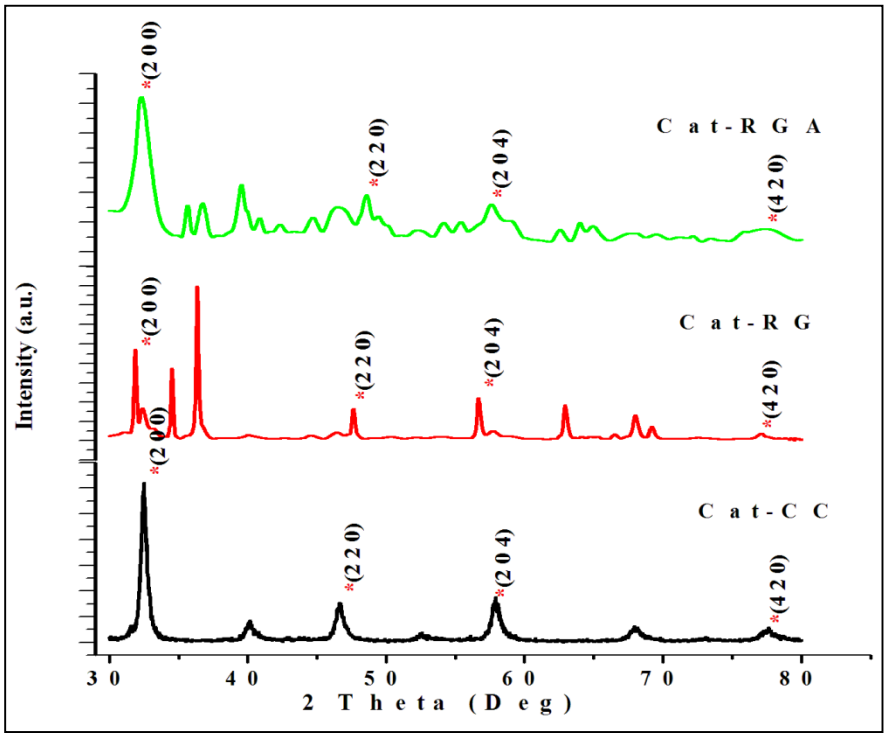

Figure 8.3 X-Ray patterns of SG and RG prepared Perovskite Catalysts

8.3.3 FTIR Characterization of the Catalysts

Figure 8.4 depicts the FTIR spectra of the catalysts in the range of 400-4000 cm^{-1}. The broader peak appeared at ~600 cm^{-1} is characteristic of the MO_6 octahedra commonly found in perovskite (ABO_3) oxide powder [Ramesh et al.1995] and is observed in this system too. The bands appeared at ~ 579 cm^{-1} and ~586 cm^{-1} in all the catalyst samples are ascribed to Fe-O and MO_6 stretch vibrations in the perovskite structure [Zhou et al. 2010]. In sol gel prepared air calcined catalyst Cat-CC and RG prepared Cat-RGA MO_6 stretch vibrations appeared at 586 cm^{-1} while in Cat-RG its shifts towards lower Wavenumbers 579 cm^{-1}. The peak shift is towards lower wave number side indicates

the mass of that molecule is increased because frequency of vibration is inversely proportional to mass of vibrating molecule so heavier the molecule, less the vibration frequency and lower the wave numbers. The peaks found at 2350 cm^{-1} in the samples are due to the presence of adsorbed atmospheric moisture as reported earlier [Mandelovici et al. 1994]. The absorption band at 1480cm^{-1} in the Cat-CC were corresponded to nitrate ion. As nitrate precursors were used for the preparation of catalyst. In addition, the band at 1100 cm^{-1} was resembled to Co-OH/Fe-OH bends which is confirmed with the reported value that MOH bending mode appears below 1200 cm^{-1} [Nakamoto 1997].

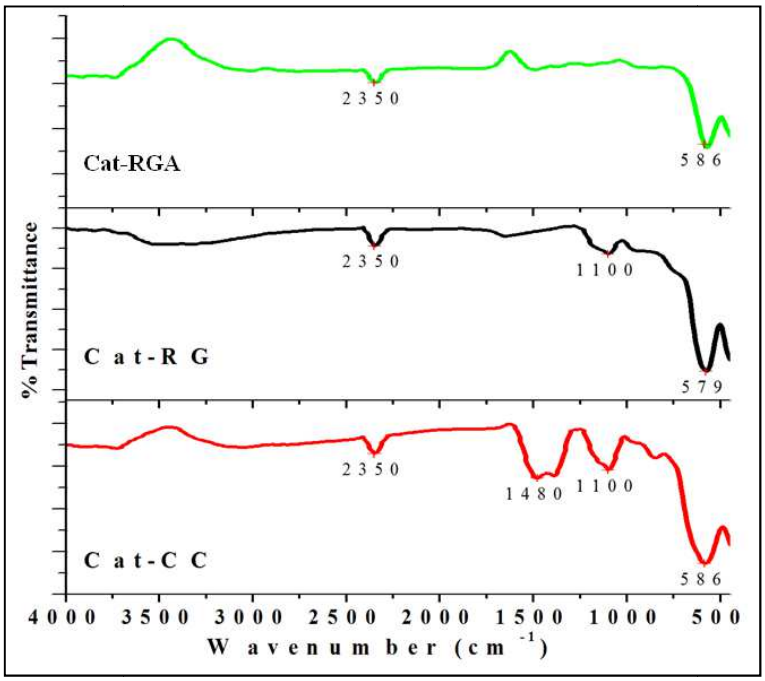

Figure 8.4 FTIR spectra of SG and RG prepared Perovskite Catalysts

8.3.4 XPS Analysis of the Catalysts

The XPS Spectra of $La_{0.9}Sr_{0.1}Co_{0.5}Fe_{0.5}O_{3-\delta}$ sample calcined in air (Cat-CC) are shown in Figure 8.5. The figure 8.5(a) shows the XPS spectra of La 3d, the peaks of La $3d_{5/2}$ and La $3d_{3/2}$ were situated at 854.2 eV and 857.4 eV, and at 837.1 eV and 840.6 eV,

respectively. The spin-orbit splitting of La 3d level is 17.0 eV. Figure 8.5 (b) and 8.5 (c) shows the XPS spectra of Co 2p and Fe 2p respectively. The spin-orbit splitting of Co 2p and Fe 2p levels are 15.2 and 12.8 eV which is in well support with the literature [Ichimura et al. 1980]. The O 1s energy spectrum consists of two peaks having binding energies 531.2 and 533.8, which correspond to two forms of oxygen, i.e. lattice oxygen and adsorption oxygen respectively as shown in figure 8.5(d).

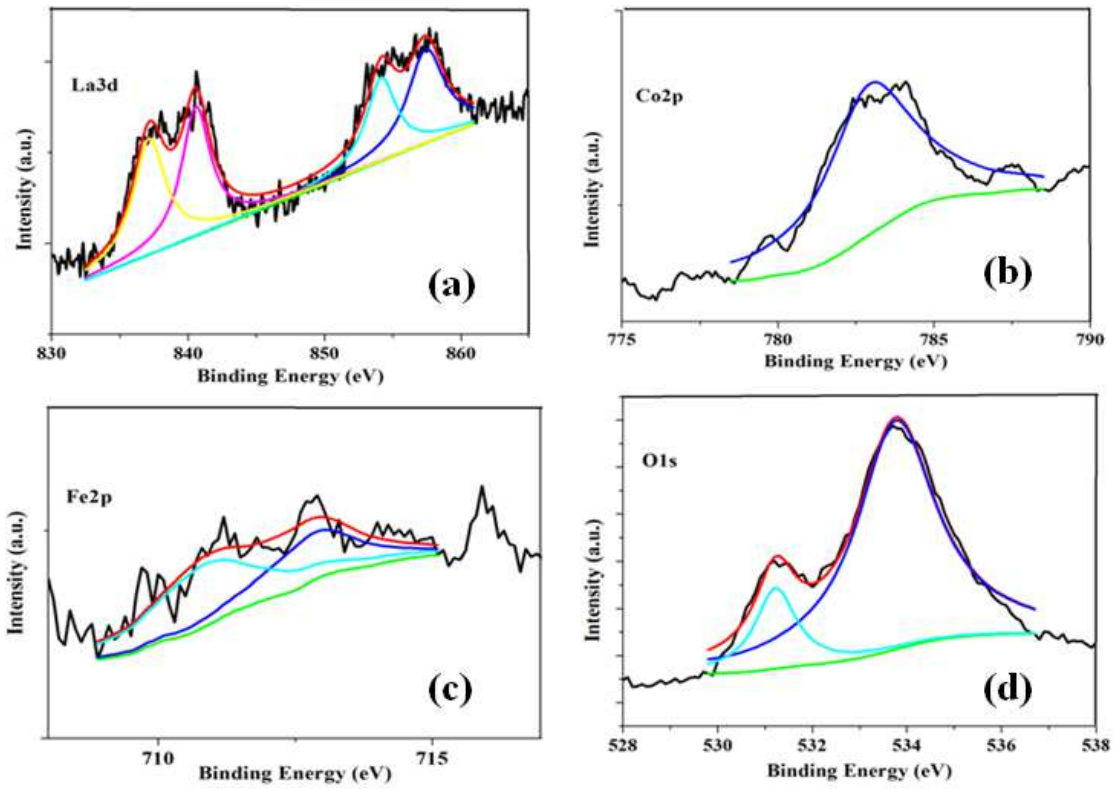

Figure 8.5 XPS Spectra of Cat-CC

The characteristic spectra of catalyst Cat-RGA are displayed in Figure 8.6, the collected data for La 3d, Co 2p, Fe 2p and O 1s. There exists relatively more adsorption oxygen on the surface indicating the presence of more oxygen vacancies. These adsorption oxygen traps electron and form more active O_2^-. Figure 8.6(a) shows the XPS spectra of La 3d, the peaks of La $3d_{5/2}$ and La $3d_{3/2}$ were situated at 853.3 eV and 856.8 eV and

at 836.4 eV and 840.4 eV, respectively. The spin-orbit splitting of La 3d level is 16.4 eV. Fig 8.6(b) and 8.6(c) shows the XPS spectra of Co 2p and Fe 2p respectively. The spin-orbit splitting of Co 2p and Fe 2p levels are 15.2 and 12.8 eV which are in well support with the literature [Ichimura et al. 1980, Cesar et al. 2000]. The O 1s energy spectrum consists of two peaks, which correspond to two forms of oxygen, i.e. lattice oxygen and adsorption oxygen are shown in figure 8.6(d). As in both the catalysts some of La^{3+} was replaced by Sr^{+}, there were changes in the relative ratio of adsorption to lattice oxygen. More adsorption oxygen existed on the surface indicating the presence of more oxygen vacancies and an increased content of quasi-free electrons in the catalyst. More adsorption oxygen traps more electrons and thus it is favourable for forming more O^{2-}, which becomes more active centres for oxidation, thus it results in the enhancement in oxidizing ability of the catalyst. It would contribute to the decrease of the combustion temperature of soot particles.

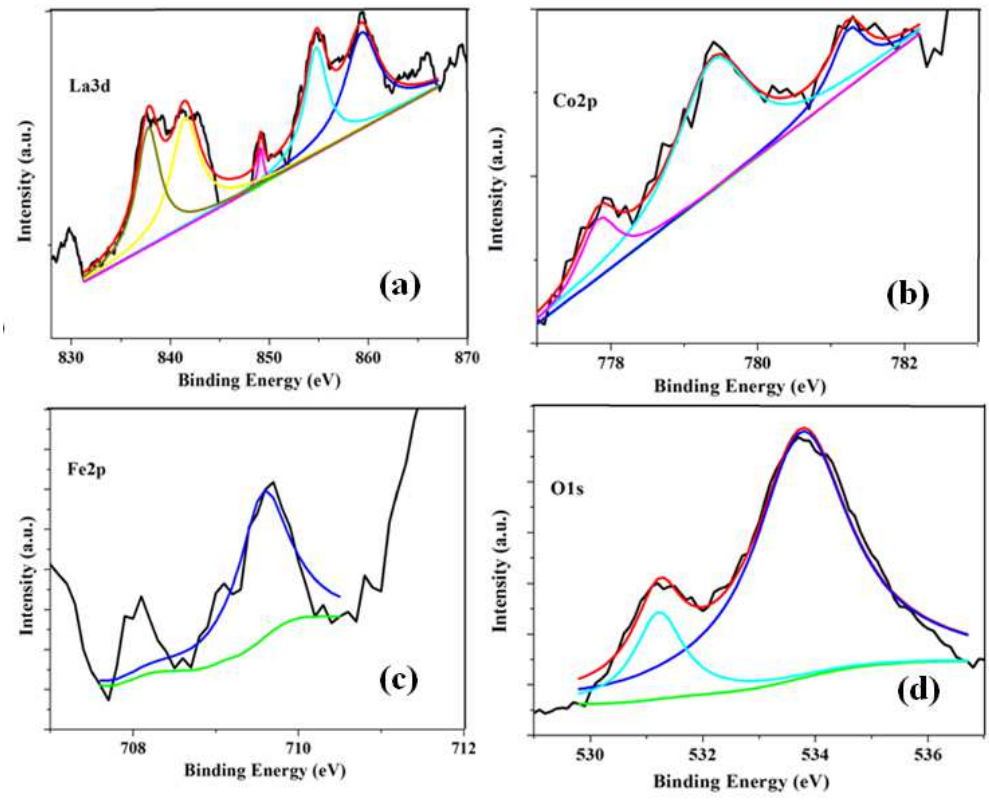

Figure 8.6 XPS Spectra of $La_{0.9}Sr_{0.1}Co_{0.5}Fe_{0.5}O_{3-\delta}$-RGA

8.3.5 SEM characterization of the Catalysts

The SEM micrographs of perovskite catalysts shown in Figure 8.7 represent quite different morphologies of the catalyst samples. It can be seen that the morphologies of particles are of irregular shape and most of them are within the nano-scale (<100 nm).

The Cat-RG, prepared by the reactive grinding, possessed granular shape particles, while the addition of ZnO entirely changed the morphology of the Cat-RGA, it may be due the interaction of the surfaces of the particles.

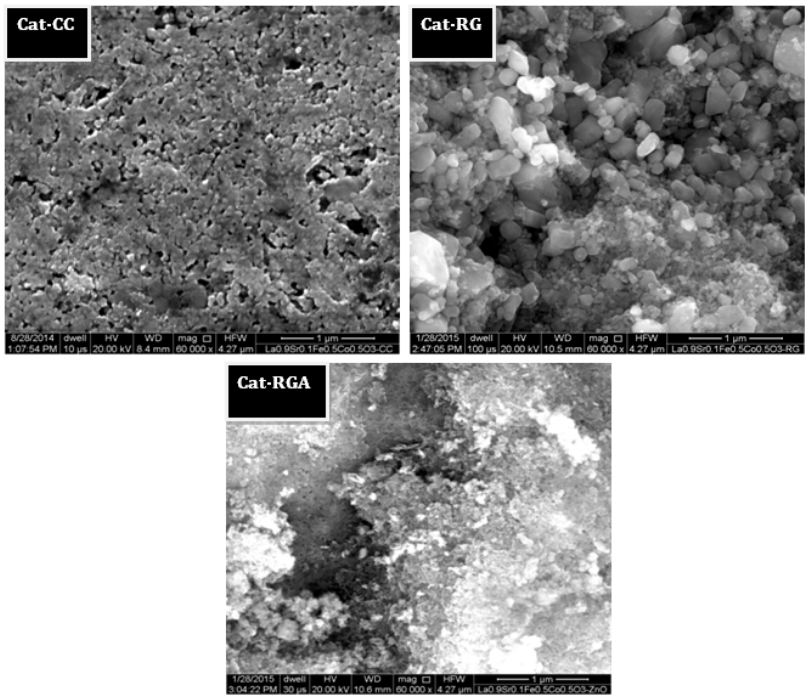

Figure 8.7 SEM images of Perovskite Catalysts

8.3.6 Energy Dispersive X-ray (EDX) of the Catalysts

It was evident from the results of energy dispersive X-ray (EDX) analysis that all the samples were pure due to presence of La, Co, Fe and O peak there is no other element present in the spectra as shown in figure 8.8. It also confirms the presence of perovskite phase in the sample which is in good harmony with the XRD and XPS experiment results. The theoretical and experimental data (atomic %) of Cat-CC and Cat-RGA are shown in table 8.3.

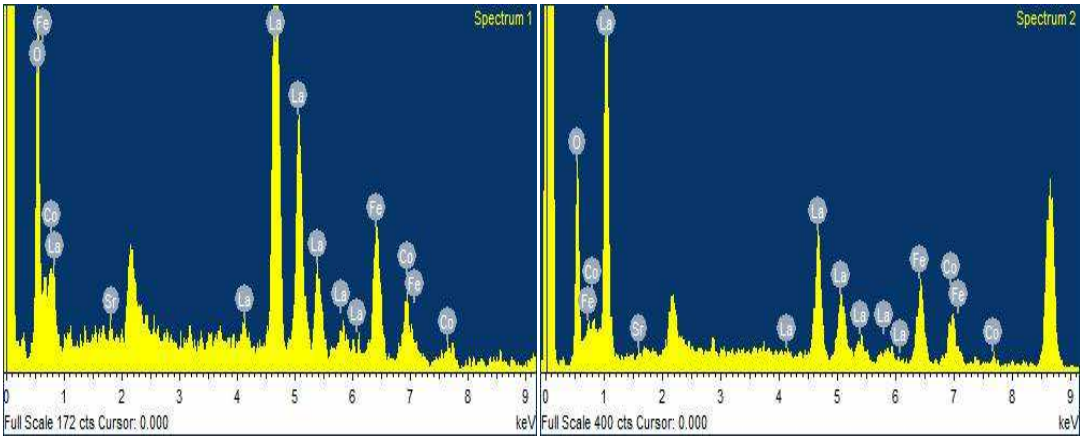

Figure 8.8 EDX spectra of (A) Cat-CC and (B) Cat-RGA perovskite catalyst

Table 8.3 Atomic % data of Cat-CC and Cat-RGA

Element	**Cat-CC (Atomic %)**		**Cat-RGA (Atomic %)**	
	Theoretical	**Experimental**	**Theoretical**	**Experimental**
O	60	57.54	60	59.23
Fe	10	09.87	10	12.00
Co	10	13.93	10	08.34
Sr	02	1.14	02	01.36
La	18	13.4	18	14.78

8.3.7 Catalytic Activity Measurements

Soot conversion as the function of temperature over prepared catalysts are shown in figure 8.9 and light off temperature on the catalyst are presented in Table 8.4. Cat-RGA exhibited highest activity for soot conversion than other two. The soot conversion of 100% was achieved with this catalyst at the lowest temperature of 324^{o}C. This may be related to unusual characteristics arisen from the severe mechano-chemical deformation during ball-milling; leading to cold welding and fractures in nano-structured catalyst.

The oxidation of diesel soot is directly dependant on three factors. The first one is the reducibility of the transition metal cations in order to produce vacancies. These vacancies are essential to allow the soot oxidation. The second factor is the amount of -

oxygen available to initiate the reaction of soot oxidation into CO_2. The third factor is crystallite size and surface area. As the crystallite size is smaller and surface area of sample is higher in a catalyst, it accommodates more active sites for soot oxidation reaction. The crystallite size is smaller and surface area is higher of Cat-RGA than Cat-CC and Cat-RG. Therefore, numbers of active sites available in Cat-RGA are more for soot oxidation reaction.

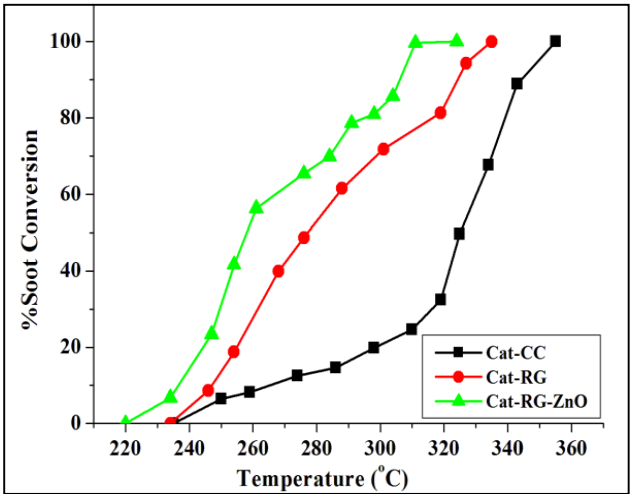

Figure 8.9 Performance of the catalysts for Diesel Soot Oxidation

Table 8.4 Characteristics Temperatures of different Catalyst samples for Soot Oxidation

Catalysts	**T_i(°C)**	**T_{50}(°C)**	**T_f(°C)**
Cat-CC	238	330	355
Cat-RG	234	277	335
Cat-RGA	220	259	324

8.3.7.1 Effect of Catalyst-Soot Contact

A loose contact study was also carried out to simulate the actual circumstances of diesel particulate filter. Figure 8.10 shows a comparison of conversion of soot particles over Cat-RC under tight and loose contacts conditions of the catalyst-soot. It can be visualized from figure 8.10 that loose contact exhibited lower activity than tight

contact. The observation is obvious as the catalysis is a surface phenomenon, higher the surface contacts (tight contact) higher the activity. From the table 8.5 it is clear that Cat-RC resulted complete soot oxidation at T_f = 372 ^oC under loose contact which is 48^oC higher than tight contact. The catalytic activity for soot oxidation under loose contact conditions is found to be very much appreciating within the diesel exhaust conditions i.e. < 450^oC. Thus, it should be effective to oxidize the soot on coating over DPF in real diesel engine exhaust.

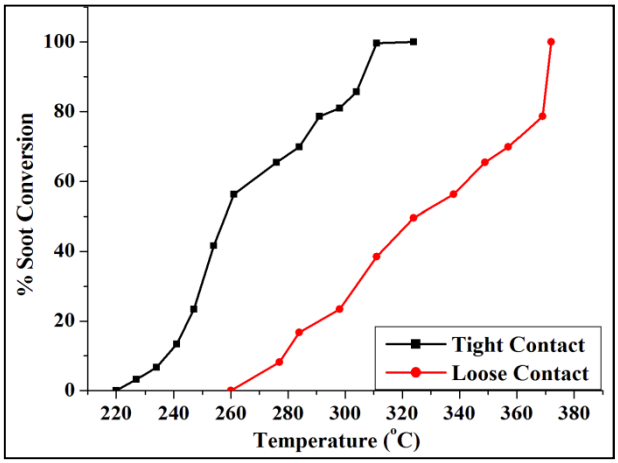

Figure 8.10 The Performance of the Cat-RGA for Diesel Soot Oxidation in Loose and Tight contact

Table 8.5 Light off Temperatures on Cat-RGA under different Catalyst-Soot Contacts

Contact Type	**T_i(^oC)**	**T_{50}(^oC)**	**T_f(^oC)**
Tight contact	220	259	324
Loose contact	260	339	372

8.3.8 Thermal stability of the Catalyst

Further, experiments were conducted to examine the thermal stability of typical Cat-RGA by consecutive soot combustion for five cycles, and the results are shown in Table 6. It is evident from the table that the catalyst maintained its high catalytic activity for repeated five cycles under the condition of tight contact between catalysts and soot

particles. The variation in the light off temperature of soot oxidation values of T_i, T_{50} and T_f are within the experimental error (table 8.6). The results indicate that the catalyst has good thermal stability for soot oxidation.

Table 8.6 Stability test of catalyst Cat-RG for Soot Combustion under Tight Contact

Test Cycle	**T_i(^oC)**	**T_{50}(^oC)**	**T_f(^oC)**
1^{st}	220	259	324
2^{nd}	221	260	325
3^{rd}	220	260	324
4^{th}	219	258	324
5^{th}	222	259	323

8.4 Conclusions

Three catalysts; Cat-CC, Cat-RG and Cat-RGA are synthesized by the sol-gel method and reactive grinding. XRD analysis confirms the perovskite structure in all the prepared catalysts consisting of nano-size crystallites.

The catalysts synthesized by RG with ZnO additive possesses the highest surface area and the smallest crystallites than ones prepared by RG method without additive as well as SG method. The RG technique also creates the Lattice defects, which increases the density of active sites in the catalyst responsible for enhanced catalyst's activity. The Cat-RGA which is inexpensive, thermally stable and have highest activity within the temperature range of diesel engine exhaust could be applied in the self-regenerative diesel particulate filter.